ACS APPLIED MATERIALS & INTERFACES

Research Article

www.acsami.org

Monolayer Ti_2CO_2: A Promising Candidate for NH_3 Sensor or Capturer with High Sensitivity and Selectivity

Xue-fang Yu,[†] Yan-chun Li,[‡] Jian-bo Cheng,[†] Zhen-bo Liu,[†] Qing-zhong Li,[†] Wen-zuo Li,[†] Xin Yang,[†] and Bo Xiao*,[†]

[†]The Laboratory of Theoretical and Computational Chemistry, School of Chemistry and Chemical Engineering, Yantai University, Yantai 264005, China

[‡]Institute of Theoretical Chemistry, Jilin University, Changchun 130021, China

Supporting Information

ABSTRACT: Ti_2C is one of the thinnest layers in MXene family with high potential for applications. In the present study, the adsorption of NH_3, H_2, CH_4, CO, CO_2, N_2, NO_2, and O_2 on monolayer Ti_2CO_2 was investigated by using first-principles simulations to exploit its potential applications as gas sensor or capturer. Among all the gas molecules, only NH_3 could be chemisorbed on Ti_2CO_2 with apparent charge transfer of 0.174 e. We further calculated the current−voltage (I−V) relation using the nonequilibrium Green's function (NEGF) method. The transport feature exhibits distinct responses with a dramatic change of I−V relation before and after NH_3 adsorption on Ti_2CO_2. Thus, we predict that Ti_2CO_2 could be a promising candidate for the NH_3 sensor with high selectivity and sensitivity. On the other hand, the adsorption of NH_3 on Ti_2CO_2 could be further strengthened with the increase of applied strain on Ti_2CO_2, while the adsorption of other gases on Ti_2CO_2 is still weak under the same strain, indicating that the capture of NH_3 on Ti_2CO_2 under the strain is highly preferred over other gas molecules. Moreover, the adsorbed NH_3 on Ti_2CO_2 could be escapable by releasing the applied strain, which indicates the capture process is reversible. Our study widens the application of monolayer Ti_2CO_2 not only as the battery material, but also as the potential gas sensor or capturer of NH_3 with high sensitivity and selectivity.

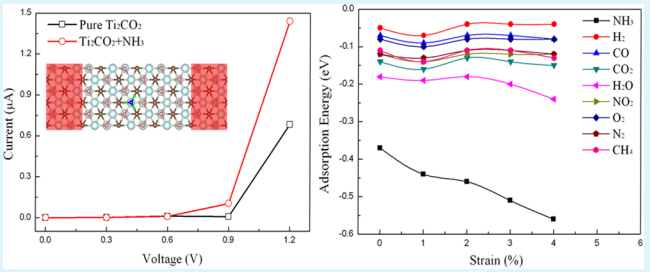

KEYWORDS: *MXene, monolayer Ti_2CO_2, NH_3 sensor, NH_3 capture, sensitivity, selectivity*

1. INTRODUCTION

NH_3 is the most common substitute for chlorofluorocarbons (CFCs) in cooling systems, and it is a toxic compound and volatile, which is very harmful to the human body.[1] On the other hand, NH_3 has been widely used to synthesize various materials in chemical industries and is a promising candidate as a future energy carrier in vehicles and as an NH_3 reservoir for the selective catalytic reduction (SCR) of NO_x gases in diesel cars and trucks.[2−6] Thus, it is highly desirable to find an effective method to sensor and capture the NH_3 gases for atmospheric environmental controls and industry applications.

Semiconducting metal oxides and low-dimension materials have been considered to be the most promising candidate for gas sensors, which is due to its advantages such as low cost, small dimensions, and great compatibility with conventional microelectromechanical processing. So far, NH_3 sensors based on metal oxides (such as SnO_2, TiO_2, In_2O_3)[7−9] and low-dimension materials (such as carbon nanocone;[10] silicon carbide nanotube;[11] Al, B, Li, N-doped carbon nanotube;[12−15] Ga, Al-doped boron nitride nanotube;[16] and Au, B-doped graphene[17,18]) have been widely studied. However, the major drawback of these sensors is the lack of selectivity to only one particular gas (NH_3), and most of these sensors show long recovery times at room temperature due to the tendency of NH_3 to strongly interact with many substrates. On the other hand, NH_3 storage has been widely studied, and it is found that the metal ammines $Mg(NH_3)_6Cl_2$,[19] $Sr(NH_3)_8Cl_2$,[20] and mixed metal halide ammines[21] could store NH_3 very effectively. However, the release of NH_3 from these materials needs either high temperature (>450 K) or multistep reactions, which are not suitable for automotive or fuel cell applications.

Very recently, MXene has attracted worldwide attention due to its structural similarity to graphene.[22,23] MXene could be obtained from the removal of "A" group layer from the MAX phase, where "M" represents an early transition metal, "X" denotes C or N, and "A" is an A-group (mostly IIIA and IVA, or groups 13 and 14) element.[22,23] Since Gogotsi et al. revealed the potential use of MXene layers as the electrochemical energy storage, such as electrode for batteries, supercapacitors, and hybrid devices,[24] several theoretical and experimental studies extensively reported the performance of MXene as anode

Received: April 29, 2015
Accepted: June 4, 2015
Published: June 4, 2015

DOI: 10.1021/acsami.5b03737
ACS Appl. Mater. Interfaces 2015, 7, 13707−13713

material for metal ion batteries, the spintronic, and the optical devices.[25−28]

Among all the MXenes, Ti_2C is one of the thinnest phases, and it is found to be terminated with several kinds of functional group, such as F, OH, and/or O in the real etching process with HF acid.[22,23] It has already been revealed that the electronic property of Ti_2C is strongly dependent on the functional group, with only Ti_2CO_2 exhibiting semiconductor character, Ti_2C, Ti_2CF_2, and $Ti_2C(OH)_2$ exhibiting metallic character.[29,30] Thus, Ti_2C with O termination may possess much more potential applications than other terminations in view of its semiconducting property.[31]

In this work, the potential of monolayer Ti_2CO_2 as the gas sensor and capture is explored by first-principle simulation. The preference adsorption of NH_3 against the other gas molecules (H_2, CH_4, CO, CO_2, N_2, NO_2 and O_2) on monolayer Ti_2CO_2 suggests the selectivity of monolayer Ti_2CO_2 toward NH_3. The distinct transport feature with a dramatic change of $I-V$ relation before and after NH_3 adsorption indicates the strong sensitivity of monolayer Ti_2CO_2 toward NH_3. More importantly, the interaction of monolayer Ti_2CO_2 with NH_3 can be tuned easily by strains, indicating the facile way of NH_3 capture and releasing using monolayer Ti_2CO_2.

2. COMPUTATIONAL METHOD

The density functional theory (DFT) calculation was performed using the Vienna Ab-Initio Simulation Package.[32,33] The electron−ion interaction was described by projector augmented-wave (PAW)[34] pseudopotentials. For the exchange and correlation functionals, we use the Perdew−Burke−Ernzerhof (PBE) version of the generalized gradient approximation (GGA).[35] The energy cutoff of 520 eV was used for the wave functions expansion. The Brillouin zone integration was sampled by with 3 × 3 × 1 k-grid mesh for geometry optimization, and 5 × 5 × 1 k-grid mesh for electronic properties calculations to achieve high accuracy. The geometries were fully optimized until the forces on each atom is less than 0.01 eV/Å. The van der Waals interaction is introduced to treat the interaction between gas molecules and the monolayer Ti_2CO_2, and it is described by a semiempirical correction by the Grimme method.[36] The periodic structure of Ti_2CO_2 monolayer (3 × 3 supercell) has been decoupled by a vacuum thickness larger than 20 Å.

The adsorption energy (E_{ads}) is defined as

$$E_{ads} = E_{Ti2CO2+Gas} - E_{Gas} - E_{Ti2CO2}$$

where $E_{Ti2CO2+Gas}$ is the total energy of monolayer Ti_2CO_2 adsorbed with gas molecule, E_{Gas} is the total energy of gas molecule, and E_{Ti2CO2} is the total energy of monolayer Ti_2CO_2.

The electron transport calculations were performed using the Atomistix ToolKit (ATK) package[37] based on the density functional theory and nonequilibrium Green's function (NEGF) method. A numerical atomic basis set, a single-ζ basis with polarization, was used to solve the Kohn−Sham equation. GGA in the PBE form was adopted for the electron−electron interactions. The K-point sampling in the direction parallel to the interface (the x and y directions) is 2 × 2, and the number of real space mesh in the z direction is 50.

3. RESULTS AND DISCUSSION

The most stable structure of O functionalized monolayer Ti_2C, as mentioned in our previous study,[28] is shown in Figure 1. The lattice parameter of Ti_2CO_2 unit cell is 3.04 Å, which is consistent with other theoretical studies.[28,29] We first consider several typical and possible adsorption sites for the gas molecules (NH_3, H_2, CH_4, CO, CO_2, N_2, NO_2, and O_2) adsorption on the monolayer Ti_2CO_2, including the top site over Ti, C, or O atom, bridge site between neighboring O and O, or Ti and O atoms. Also, several typical orientation of gas molecules with respective to the monolayer Ti_2CO_2 surface are considered. Taking NH_3 molecule's adsorption as an example, NH_3 molecule is initially placed vertically (including $Ti_2CO_2 \leftrightarrow H-NH_2$, and $Ti_2CO_2 \leftrightarrow H_2-NH$) or parallel (including $Ti_2CO_2 \leftrightarrow N-H_3$, and $Ti_2CO_2 \leftrightarrow H_3-N$) to the surface of monolayer Ti_2CO_2 for all the studied adsorption sites, and in each case, all the typical orientation of NH_3 molecules are considered.

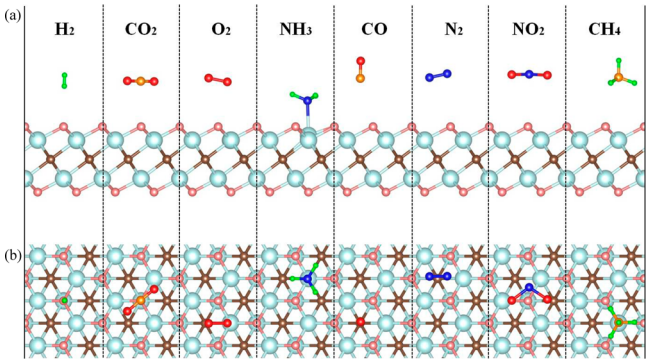

Figure 1. A schematic illustration of (a) side, and (b) top view of the adsorption of NH_3, H_2, CH_4, CO, CO_2, N_2, NO_2, or O_2 molecule on monolayer Ti_2CO_2.

The most stable structures for the adsorption of gas molecules on monolayer Ti_2CO_2 are shown in Figure 1, and the corresponding adsorption energies, charge transfers, and the nearest distance between gas molecules and Ti_2CO_2 sheet (denote as $d_{Gas-T2CO2}$) are listed in Table 1. In the case of NH_3 molecule, the strongest binding site is found to be the former with the N atom located directly above the Ti atom in Ti_2CO_2, as shown in Figure 1. This structure has the adsorption energy of −0.37 eV and a charge transfer of 0.174 e from the NH_3 to the Ti_2CO_2. The as-formed N−Ti bond length is 2.35 Å. Furthermore, the NH_3 adsorption induces a locally structural deformation to both NH_3 molecule and Ti_2CO_2. The dihedral angle of H−H−H−N in NH_3 decreases from 39.50° in free NH_3 to 35.42° in the adsorbed form. The NH_3-adsorbed Ti atom is pulled outward from the layer with its neighboring Ti−C bond length increase from 2.08 to 2.35 Å. The three O atoms adjacent to N atom have slightly moved away from its original position due to the repulsion between O atoms and N atoms. The local structure deformation together with the charge transfer indicates the strong interaction of NH_3 with monolayer

Table 1. Adsorption Energy (E_{ads}), the Charge Transfer (C_T) from Gas Molecule to Ti_2CO_2, and the Nearest Distance ($d_{Gas-Ti2CO2}$) between Gas Molecule and Ti_2CO_2

gas molecules	E_{ads} (eV)	C_T (e)[a]	$d_{Gas-Ti2CO2}$ (Å)
NH_3	−0.37	0.174	2.35
H_2	−0.05	0.003	2.76
CO	−0.07	0.004	3.19
CO_2	−0.14	−0.007	3.08
NO_2	−0.12	−0.003	3.35
O_2	−0.08	−0.003	3.46
N_2	−0.12	−0.002	3.71
CH_4	−0.11	−0.001	3.06

[a]A positive C_T value indicates a transfer of electrons from the gas molecule to Ti_2CO_2.

DOI: 10.1021/acsami.5b03737
ACS Appl. Mater. Interfaces 2015, 7, 13707−13713

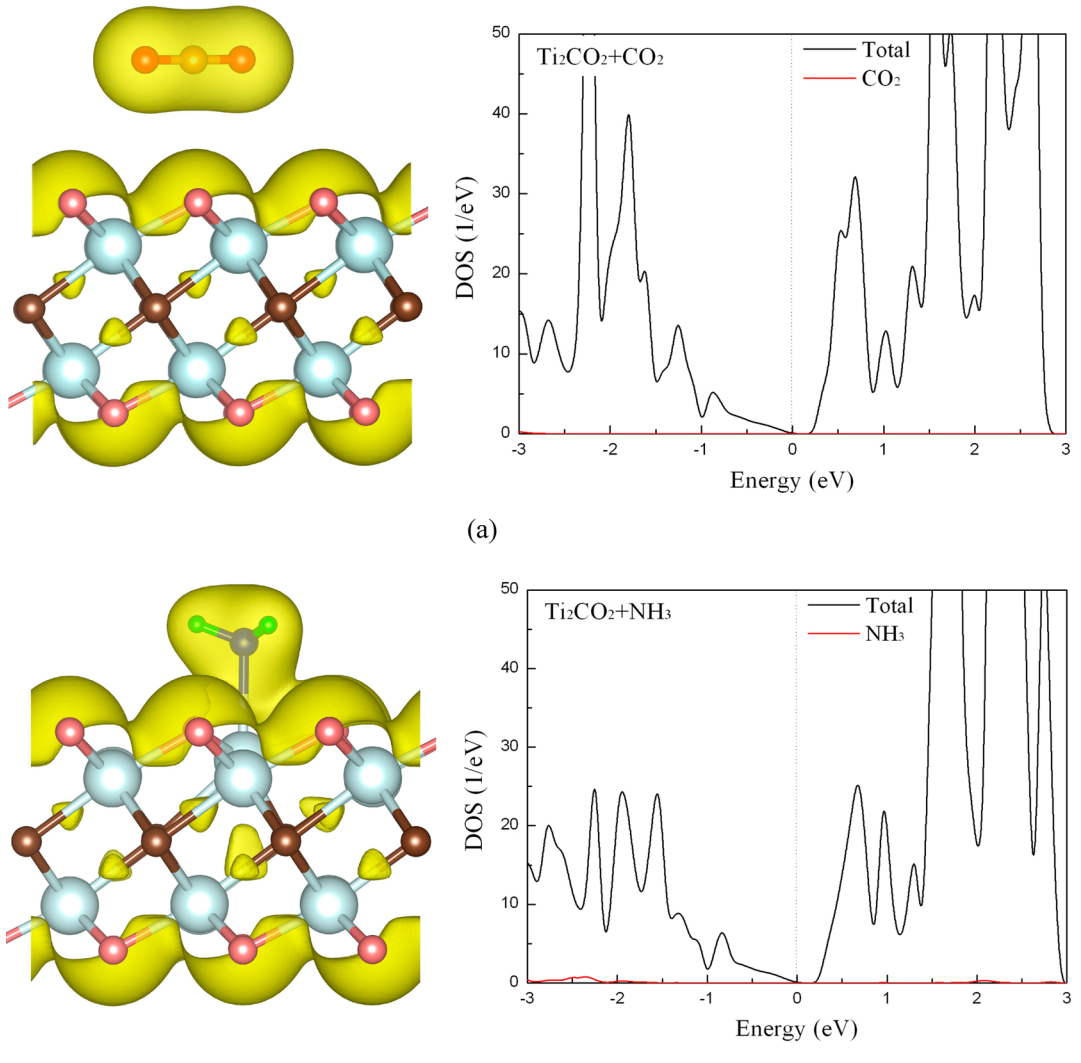

Figure 2. Total charge density and the density of states of (a) CO_2 and (b) NH_3 adsorption on monolayer Ti_2CO_2.

Ti_2CO_2, which is very consistent with the small adsorption energy.

In contrast, other gas molecules (H_2, CH_4, CO, CO_2, N_2, NO_2, and O_2) exhibit quite different adsorption behavior compared with the case of NH_3. As shown in Table 1, the adsorption energies of these gas molecules on monolayer Ti_2CO_2 range from −0.05 to −0.14 eV, and the charge transfers between gas molecules and monolayer Ti_2CO_2 are from −0.007 to 0.004 e, which are obviously smaller than that in the case of NH_3 (adsorption energy −0.37 eV, and charge transfer 0.174 e). As shown in Figure 1, the adsorption of these gas molecules has a relatively large $d_{Gas-T2CO2}$ value and the change in the structures of gas molecules and Ti_2CO_2 is negligible, which implies the weak interaction between them. In detail, as shown in Figure 1, H_2 (or CO) molecule tends to be vertically adsorbed on the O (or C) site of Ti_2CO_2. The $d_{H2(or\ CO)-T2CO2}$ and the adsorption energy is 2.76 (or 3.19) Å and −0.05 (or −0.07) eV, respectively; CO_2 (or NO_2) molecule prefers to adsorb on the O site of Ti_2CO_2, and the O−C−O (or O−N−O) bond is parallel to the Ti_2CO_2 sheet, the $d_{CO2(or\ NO2)-T2CO2}$ and the adsorption energy are 3.08 (or 3.35) Å and −0.14 (or −0.12) eV, respectively; O_2 (or N_2) molecule prefers to adsorb on the O site of Ti_2CO_2 sheet with a tilt structure, the $d_{O2(or\ N2)-T2CO2}$ and the adsorption energy are 3.46 (or 3.70) Å and −0.08 (or −0.12) eV, respectively. Lastly, CH_4 molecule tends to be adsorbed on the O-site with one C−H bond perpendicular to the surface of Ti_2CO_2 sheet while the other three C−H bonds point to the O atoms. The calculated $d_{CH4-T2CO2}$ and the adsorption energy are 3.06 Å and −0.11 eV, respectively.

To analyze the electronic interaction between the gas molecules and Ti_2CO_2 sheet, we calculate the density of state (DOS) and total charge density. Taking the adsorption of NH_3 and CO_2 on Ti_2CO_2 as examples, in the case of CO_2, the total charge density (Figure 2a) shows no overlap between CO_2 and Ti_2CO_2, indicating the weak interaction between them, and correspondingly the change in the DOS of Ti_2CO_2 is negligible as shown in Figure 2a. Similar results also could be found in the case of the other gas molecules (including H_2, CH_4, CO, N_2, NO_2, and O_2). In view of the weak interaction and the few charge transfer between Ti_2CO_2 and these gas molecules (including H_2, CH_4, CO, CO_2, N_2, NO_2, and O_2), Ti_2CO_2 could not be the sensor to these gas molecules. In contrast, in the case of NH_3, the electronic charge are strongly overlapped,

DOI: 10.1021/acsami.5b03737
ACS Appl. Mater. Interfaces 2015, 7, 13707−13713

as shown in Figure 2b, leading to orbital mixing and large charge transfer. The adsorption of NH_3 induces several distinct states at the lower-lying valence bands in the energy range around −2.5 eV; however, there is no noticeable modifications of the DOS near Fermi level (E_F), as shown in Figure 2b. Thus, the adsorption of NH_3 does not have a substantial effect on the electronic structure of monolayer Ti_2CO_2. It should be noted that the adsorption-induced charge transfer is expected to affect the resistivity of the system, which can be measured experimentally and could be a marker for gas sensors. The evidence could be found in detecting NH_3 molecule by using MoS_2 and phosphorene,[38,39] where the resistivity of the system increases obviously after the adsorption of NH_3 due to the relatively large charge transfer between them, although the change in the electronic properties of system is negligible.

To quantitatively evaluate the performance of monolayer Ti_2CO_2 as the NH_3 sensor, we simulated the current−voltage (I−V) relations before and after the NH_3 adsorption using the NEGF method, which allows the monitoring of the resistivity change in sensing materials upon the adsorption of chemicals. Ti_2CO_2-based sensor is simulated using a model consisting of a Ti_2CO_2 sheet contacted by two Ti_2CO_2 electrodes, as shown in Figure 3a. The I−V curves for such Ti_2CO_2 junctions with and

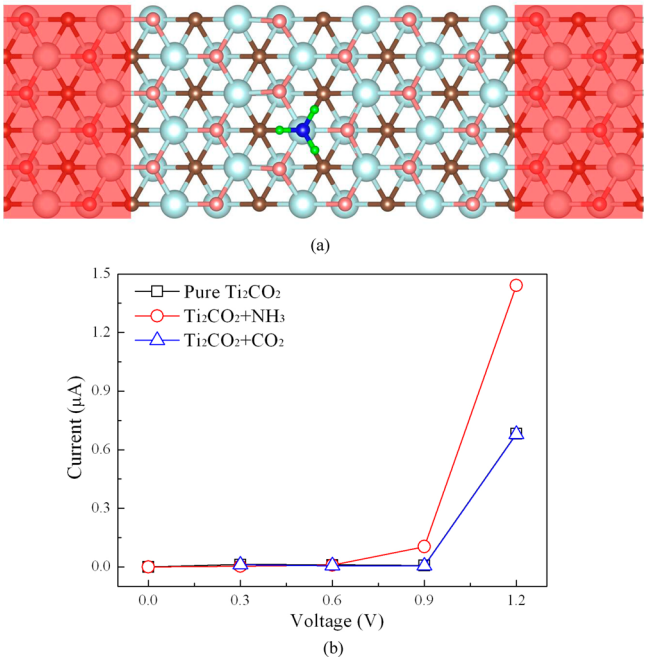

Figure 3. (a) A schematic illustration of Ti_2CO_2-based sensor for detecting NH_3 molecule; (b) the current−voltage (I−V) relations before and after the adsorption of NH_3 or CO_2 molecule on monolayer Ti_2CO_2.

without the adsorption of NH_3 molecule is shown in Figure 3b. The I−V curves of Ti_2CO_2 exhibits a clear nonlinear behavior. After the adsorption of NH_3 molecule, a dramatic increase of current is observed when the applied bias voltage larger than 0.9 V, indicating the high sensitivity of Ti_2CO_2 sensor to NH_3. In detail, the current passing through the monolayer Ti_2CO_2 is 0.68 μA under the bias voltage of 1.2 V, but with the adsorption of NH_3 molecule, the current under the same bias is increased to 1.44 μA, which is about the 111% increase. The increase in the current indicates the decrease of resistance after the NH_3 adsorption, which could be directly measured in experiment. As a comparison, the I−V curves before and after the adsorption of CO_2 molecule on Ti_2CO_2 have been calculated as shown in Figure 3b. In this case, the current change is negligible with the increase of applied bias voltage, and the main reason may result from the little charge transfer (−0.007 e) between them. Similar I−V character is also expected to occur when the other gas molecules (i.e., H_2, CH_4, CO, N_2, NO_2 and O_2) adsorb on Ti_2CO_2 due to the same reason. This result further confirms the high selectivity of Ti_2CO_2 as the NH_3 sensor. In view of the dramatically increased current value after the NH_3 adsorption on Ti_2CO_2, together with the relatively large charge transfer (0.174 e) between NH_3 and Ti_2CO_2 as compared with other gas molecules (from −0.007 to 0.004 e), we predict that monolayer Ti_2CO_2 is a promising candidate to sensor NH_3 molecule with high sensitivity and selectivity. It should be noted that the adsorption energy of NH_3 on Ti_2CO_2 is −0.37 eV, which is suitable for adsorption/desorption of gases on/from Ti_2CO_2 surface, and thus, the Ti_2CO_2 sensor could recover easily after detecting NH_3.

As mentioned above, MoS_2 and phosphorene have been proposed to be the NH_3 sensors.[38,39] In this work, we also theoretically estimate the performance of MoS_2 and phosphorene as the NH_3 sensor in comparison with Ti_2CO_2. To do so, we have initially considered all the possible structures for the adsorption of NH_3 on MoS_2 and phosphorene, and the corresponding most stable structures are very similar to the previous studies.[38,40] The calculated adsorption energies and the charge transfers between NH_3 and MoS_2 (and phosphorene) are listed in Table 2. These results are very consistent with

Table 2. Adsorption Energy (E_{ads}) and Charge Transfer (C_T) from NH_3 Molecule to Different 2D Materials

gas molecules	E_{ads} (eV)	C_T (e)[a]
Ti_2CO_2	−0.37	0.174
$Ti_2C(OH)_2$	−0.48	−0.117
$Ti_3C_2O_2$	−0.34	0.166
V_2CO_2	−0.81	0.265
phosphorene	−0.21	0.028
MoS_2	−0.16	0.040

[a]A positive C_T value indicates a transfer of electrons from the NH_3 molecule to 2D materials.

previous studies.[38,40] Similar to the case of Ti_2CO_2, the electronic properties of MoS_2 and phosphorene after the adsorption of NH_3 are not substantially changed,[38,40] and thus, the adsorption-induced charge transfer could act as a marker for gas sensors. It is found that the charge transfer from NH_3 to MoS_2 (0.040 e) or phosphorene (0.028 e) is obviously smaller than that in the case of Ti_2CO_2 (0.174 e). Correspondingly, the calculated I−V curve (Figure 4) before and after the adsorption of NH_3 on MoS_2 or phosphorene shows less current change as compared with the case in Ti_2CO_2, which implies the superior sensitivity of Ti_2CO_2 as the NH_3 sensor as compared with MoS_2 and phosphorene. It should be noted that the adsorption energy of NH_3 on MoS_2 or phosphorene is smaller than that of Ti_2CO_2, and thus, shorter recovery time is needed in MoS_2 or phosphorene compared with the one in Ti_2CO_2 after detecting NH_3.

As we know, Ti_2CO_2 is one of the members among MXene family.[22,23] It would be very helpful to learn about the adsorption of NH_3 molecule on other kinds of MXenes with different surface terminations (i.e., $Ti_2C(OH)_2$), structures (i.e.,

DOI: 10.1021/acsami.5b03737
ACS Appl. Mater. Interfaces 2015, 7, 13707−13713

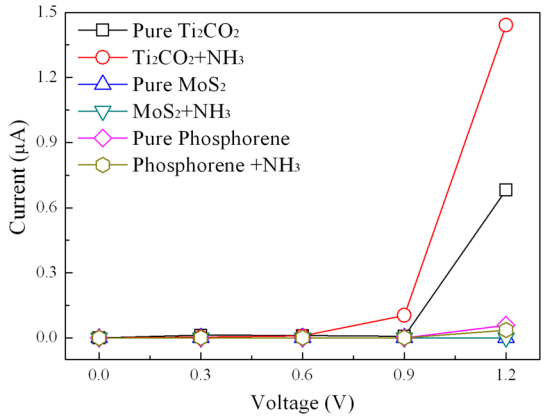

Figure 4. Calculated *I*–*V* curve before and after the adsorption of NH_3 on Ti_2CO_2, MoS_2, and phosphorene.

$Ti_3C_2O_2$), and transition metals (i.e., V_2CO_2). To do so, we have considered all the possible structures for adsorption of NH_3 molecule on monolayer $Ti_2C(OH)_2$, $Ti_3C_2O_2$ and V_2CO_2, and the corresponding most stable structures are shown in Figure S1 in the Supporting Information. For the adsorption of NH_3 on $Ti_2C(OH)_2$, the N atom of NH_3 is located directly on the top of H atom in $Ti_2C(OH)_2$ in the most stable structure, while for the adsorption of NH_3 on $Ti_3C_2O_2$ or V_2CO_2, the most stable structure is similar to the case in Ti_2CO_2, where the N atom of NH_3 adsorb on the top of transition metal (Ti or V). The corresponding adsorption energy and charge transfer values are listed in Table 2. It is found that the absolute values of charge transfer in all the above cases are larger than 0.117 e, which indicates the strong interaction of NH_3 with them. As mentioned above, the large charge transfer values could be measured experimentally and could be a marker for gas sensors. While the larger adsorption energy of NH_3 on $Ti_2C(OH)_2$ (−0.48 eV) or V_2CO_2 (−0.81 eV) implies the longer recover time after detecting NH_3, compared with NH_3 absorption on Ti_2CO_2. In the case of NH_3 adsorption on $Ti_3C_2O_2$, due to the surface structural similarity between Ti_2CO_2 and $Ti_3C_2O_2$, both the adsorption energy and the charge transfer between NH_3 and $Ti_3C_2O_2$ are very close to the ones in NH_3 absorption on Ti_2CO_2, and thus, it is expected that the $Ti_3C_2O_2$ could be another promising candidate for NH_3 sensor.

Next, we consider the possibility of Ti_2CO_2 as the capturer for NH_3 gas. As mentioned above, the adsorption energy of NH_3 on monolayer Ti_2CO_2 is −0.37 eV. According to Guo et al., the adsorption energy should be greater than −0.50 eV to effectively capture gas molecule on solid surface.[41] Thus, the perfect monolayer Ti_2CO_2 is unsuitable for NH_3 gas capture due to its relatively small adsorption energy (−0.37 eV). As shown in Figure 2b, after the adsorption of NH_3 on Ti_2CO_2, the charge transfer mainly occurs between the N atom of NH_3 and Ti atom of Ti_2CO_2, and thus, the modification of charge state on N or Ti atom might result in the change of adsorption energy. On the other hand, our previous study showed that the charge state on Ti atom of Ti_2CO_2 decreases with the increase of the applied strains.[28] Thus, we assume that more electrons might transfer from the N of NH_3 to the Ti of Ti_2CO_2 after NH_3 adsorption to compensate the decreased electrons on the Ti atom of monolayer Ti_2CO_2 if strain is applied; consequently, the adsorption of NH_3 molecule on Ti_2CO_2 might be further strengthened after applying strains.

To verify this ideal, the adsorption of gas molecules on monolayer Ti_2CO_2 with biaxial strains (from 1 to 4%) have been studied, where the strain is defined as $\varepsilon = (a - a_0)/a_0$, where a_0 and a are the lattice parameter of the unit cell without strain and strain, respectively. As shown in Figure 5, the

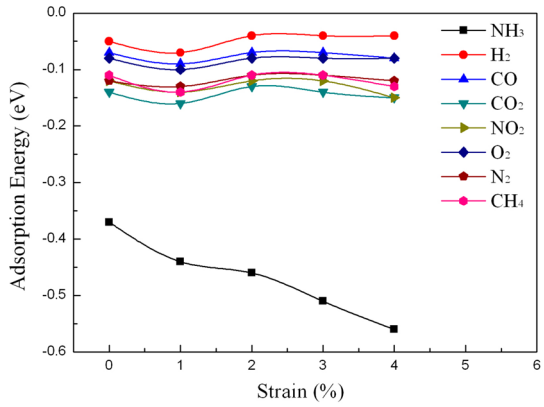

Figure 5. Adsorption energies of gas molecules (including NH_3, H_2, CH_4, CO, CO_2, N_2, NO_2, or O_2) on monolayer Ti_2CO_2 as a function of applied biaxial strains (from 0 to 4%).

adsorption energy of NH_3 on Ti_2CO_2 dramatically decreases with the increase of applied biaxial strains on Ti_2CO_2. For example, the adsorption energy becomes −0.51 eV when 3% biaxial strain is applied. Taking the adsorption energy of −0.50 eV as the reference[41] for the gas capturer, our results reveal that the NH_3 gas could be effectively captured on monolayer Ti_2CO_2 with the biaxial strains larger than 3%. In contrast, the adsorption energies of other gas molecules on Ti_2CO_2 only change slightly after applying biaxial strains, and the interaction between them is still very weak, indicating that the capture of NH_3 on monolayer Ti_2CO_2 under the biaxial strain is highly preferred over other gas molecules. Moreover, the capture of NH_3 on monolayer Ti_2CO_2 is reversible, that is, the adsorbed NH_3 can be released by releasing the applied biaxial strains. Thus, we predict that the monolayer Ti_2CO_2 could be a promising material for efficient NH_3 capture, separation, and storage. It should be noted that the sensitive strain dependence behavior also has been reported in the adsorption of NH_3 molecules on monolayer MoS_2.[42]

Finally, we present the simulated X-ray diffraction (XRD) patterns and constant-current scanning tunneling microscopy (STM) for the Ti_2CO_2 structure before and after NH_3 adsorption, as shown in Figure S2 (Supporting Information). In XRD patterns (Figure S2a, Supporting Information), the first and second strong peaks are located between the diffraction angle 0 and 10°, and the intensity of the second peak decrease slightly after the NH_3 adsorption. In Figure S2b (Supporting Information), the STM images are simulated around the Fermi level E_F (ranging from E_F −0.5 eV to E_F), employing the Tersoff–Hamann approach.[43] It is found that the bright protrusion appears after the adsorption of NH_3 on Ti_2CO_2, which is contributed from NH_3 molecule. All these results can provide useful information for future experimental studies for identifying the structure from the experimental samples.

4. CONCLUSION

By using first-principle simulation, we show that Ti_2CO_2 could be a promising candidate for the NH_3 sensor with high

DOI: 10.1021/acsami.5b03737
ACS Appl. Mater. Interfaces 2015, 7, 13707–13713

selectivity and sensitivity, which is deduced on the basis of the following evidence: (1) only NH_3 could be chemisorbed on the monolayer Ti_2CO_2 as compared with other gas molecules (H_2, CH_4, CO, CO_2, N_2, NO_2, and O_2); (2) the adsorption energy of NH_3 on Ti_2CO_2 is −0.37 eV, which is suitable for adsorption/desorption of gases on/from solid surface, and thus, the Ti_2CO_2 sensor could recover easily after detecting NH_3; (3) the electronic conductivity of Ti_2CO_2 has been significantly enhanced after the adsorption of NH_3, leading to the high sensitivity of the Ti_2CO_2 sensor to NH_3. In addition, the interaction between NH_3 and Ti_2CO_2 could be further enhanced by applying strains on Ti_2CO_2, that is, the adsorption energy becomes −0.51 eV when 3% strain is applied, while the adsorption of other gases on Ti_2CO_2 is much weaker than that of NH_3 under the same strain. Thus, our results show that Ti_2CO_2 could be used as the NH_3 capture, separation, and storage material by controlling strains.

■ ASSOCIATED CONTENT

Supporting Information

Structure and total charge density for the adsorption of NH_3 on $Ti_2C(OH)_2$, $Ti_3C_2O_2$, and V_2CO_2 sheet; simulated XRD pattern and STM for the Ti_2CO_2 structure before and after NH_3 adsorption. The Supporting Information is available free of charge on the ACS Publications website at DOI: 10.1021/acsami.5b03737.

■ AUTHOR INFORMATION

Corresponding Author

*E-mail: xiaoboy8@gmail.com.

Notes

The authors declare no competing financial interest.

■ ACKNOWLEDGMENTS

This work was partially supported by the Natural Science Foundation of Shandong Province (no. ZR2013BM016). A part of the computation in this work has been done using the Supercomputing Environment of Chinese Academy of Sciences.

■ REFERENCES

(1) Licyayo, D. C. M.; Suzuki, A.; Matsumoto, M. Interactions Among Ammonia Fungi on MY Agar Medium with Varying pH. *Mycoscience* **2007**, *48*, 20−28.

(2) Christensen, C. H.; Johannessen, T.; Sorensen, R. Z.; Norskov, J. K. Towards An Ammonia-Mediated Hydrogen Economy? *Catal. Today* **2006**, *111*, 140−144.

(3) Chakraborty, D.; Petersen, H. N.; Elkjaer, C.; Cagulada, A.; Johannessen, T. Solid Ammonia As Energy Carrier: Current Status and Future Prospects. *Fuel Cells Bull.* **2009**, *2009*, 12−15.

(4) Lan, R.; Irvine, J. T. S.; Tao, S. Ammonia and Related Chemicals As Potential Indirect Hydrogen Storage Materials. *Int. J. Hydrogen Energy* **2012**, *37*, 1482−1494.

(5) Schuth, F.; Palkovits, R.; Schlogl, R.; Su, D. S. Ammonia as a Possible Element in an Energy Infrastructure: Catalysts for Ammonia Decomposition. *Energy Environ. Sci.* **2012**, *5*, 6278−6289.

(6) Elmoe, T. D.; Sorensen, R. Z.; Quaade, U.; Christensen, C. H.; Norskov, J. K.; Johannessen, T. A High-Density Ammonia Storage/Delivery System Based on $Mg(NH_3)_6Cl_2$ for SCR-DeNO$_x$ in Vehicles. *Chem. Eng. Sci.* **2006**, *61*, 2618−2625.

(7) Wang, Y. D.; Wu, X. H.; Su, Q.; Li, Y. F.; Zhou, Z. L. Ammonia-Sensing Characteristics of Pt and SiO_2 Doped SnO_2 Materials. *Solid-State Electron.* **2011**, *45*, 347−350.

(8) Shimizu, Y.; Okamato, T.; Takao, Y.; Egashira, M. Desorption Behavior of Ammonia from TiO_2 Based Specimens-Ammonia Sensing Mechanism of Double Layer Sensors with TiO_2 Based Catalyst Layers. *J. Mol. Catal.* **2000**, *155*, 183−191.

(9) Guo, P.; Pan, H. Selectivity of Ti-Doped In_2O_3 Ceramics as An Ammonia Sensor. *Sens. Actuators, B* **2006**, *114*, 762−767.

(10) Baei, M. T.; Peyghan, A. A.; Bagheri, Z. Carbon Nanocone as an Ammonia Sensor: DFT Studies. *Struct Chem.* **2013**, *24*, 1099−1103.

(11) Ganji, M. D.; Seyed-Aghaei, N.; Taghavi, M. M.; Rezvani, M.; Kazempour, F. Ammonia Adsorption on SiC Nanotubes: A Density Functional Theory Investigation. *Fullerenes, Nanotubes, Carbon Nanostruct.* **2011**, *19*, 289−299.

(12) Azizi, K.; Karimpanah, M. Computational Study of Al- or P-doped Single-Walled Carbon Nanotubes as NH_3 and NO_2 Sensors. *Appl. Surf. Sci.* **2013**, *285P*, 102−109.

(13) Bai, L.; Zhou, Z. Computational Study of B- or N-Doped Single-Walled Carbon Nanotubes as NH_3 and NO_2 Sensors. *Carbon.* **2007**, *45*, 2105−2110.

(14) Goudarzi, F.; Vaezi, M. R.; Kazemzadeh, A. A Novel Single Wall Carbon Nanotubes-Based Sensor Doped with Lithium for Ammonia Gas Detection. *J. Ceram. Process. Res.* **2012**, *13*, 612−616.

(15) Battie, Y.; Ducloux, O.; Thobois, P.; Susi, T.; Kauppinen, E. I.; Loiseau, A. Selective Differential Ammonia Gas Sensor Based On N-Doped SWCNT Films. *Phys. Status Solidi B* **2011**, *248*, 2462−2466.

(16) Soltani, A.; Raz, S. G.; Rezaei, V. J.; Khalaji, A. D.; Savar, M. Ab Initio Investigation of Al- and Ga-Doped Single-Walled Boron Nitride Nanotubes as Ammonis Sensor. *Appl. Surf. Sci.* **2012**, *263*, 619−625.

(17) Gautam, M.; Jayatissa, A. H. Ammonia Gas Sensing Behavior of Graphene Surface Decorated with Gold Nanoparticles. *Solid-State Electron.* **2012**, *78*, 159−165.

(18) Zhang, Y. H.; Chen, Y. B.; Zhou, K. G.; Liu, C. H.; Zeng, J.; Zhang, H. L.; Peng, Y. Improving Gas Sensing Properties of Graphene by Introducing Dopants and Defects: A First-Principles Study. *Nanotechnology.* **2009**, *20*, 185504−185511.

(19) Sorensen, R. Z.; Hummelshoj, J. S.; Klerke, A.; Reves, J. B.; Vegge, T.; Norskov, J. K.; Christensen, C. H.; Sorensen, R. Z.; Hummelshoj, J. S.; Norskov, J. K. Indirect, Reversible High-Density Hydrogen Storage in Compact Metal Ammine Salts. *J. Am. Chem. Soc.* **2008**, *130*, 8660−8668.

(20) Lysgaard, S.; Ammitzboll, A. L.; Johnsen, R. E.; Norby, P.; Quaade, U. J.; Vegge, T. Resolving the Stability and Structure of Strontium Chloride Amines from Equilibrium Pressures, XRD and DFT. *Int. J. Hydrogen Energy.* **2012**, *37*, 18927−18936.

(21) Jensen, P. B.; Lysgaard, S.; Quaade, U. J.; Vegge, T. Designing Mixed Metal Halide Ammines for Ammonia Storage Using Density Functional Theory And Genetic Algorithms. *Phys. Chem. Chem. Phys.* **2014**, *16*, 19762−19740.

(22) Naguib, M.; Mochalin, V. N.; Barsoum, M. W.; Gogotsi, Y. 25th Anniversary Article: MXenes: A New Family of Two-Dimensional Materials. *Adv. Mater.* **2014**, *26*, 992−1005.

(23) Naguib, M.; Gogotsi, Y. Synthesis of Two-Dimensional Materials by Selective Extraction. *Acc. Chem. Res.* **2015**, *48*, 128−135.

(24) Lukatskaya, M. R.; Mashtalir, O.; Ren, C. E.; Dall'Agnese, Y.; Rozier, P.; Taberna, P. L.; Naguib, M.; Simon, P.; Barsoum, M. W.; Gogotsi, Y. Cation Intercalation and High Volumetric Capacitance of Two-Dimensional Titanium Carbide. *Science* **2013**, *341*, 1502−1505.

(25) Yu, X. F.; Cheng, J. B.; Liu, Z. B.; Li, Q. Z.; Li, W. Z.; Yang, X.; Xiao, B. Mg Intercalation into Ti_2C Building Block. *Chem. Phys. Lett.* **2015**, *629*, 36−39.

(26) Xie, Y.; Naguib, M.; Mochalin, V. N.; Barsoum, M. W.; Gogotsi, Y.; Yu, X.; Nam, K.-W.; Yang, X.-Q.; Kolesnikov, A. I.; Kent, P. R. Role of Surface Structure on Li-Ion Energy Storage Capacity of Two Dimensional Transition Metal Carbides. *J. Am. Chem. Soc.* **2014**, *136*, 6385−6394.

(27) Peng, X.; Peng, L.; Wu, C.; Xie, Y. Two Dimensional Nanomaterials for Flexible Supercapacitors. *Chem. Soc. Rev.* **2014**, *43*, 3303−3323.

DOI: 10.1021/acsami.5b03737
ACS Appl. Mater. Interfaces 2015, 7, 13707−13713

(28) Yu, X. F.; Cheng, J. B.; Liu, Z. B.; Li, Q. Z.; Li, W. Z.; Yang, X.; Xiao, B. The Band Gap Modulation of Monolayer Ti_2CO_2 by Strain. *RSC Adv.* **2015**, *5*, 30438−30444.
(29) Khazaei, M.; Arai, M.; Sasaki, T.; Chung, C.-Y.; Venkataramanan, N. S.; Estili, M.; Sakka, Y.; Kawazoe, Y. Novel Electronic and Magnetic Properties of Two-Dimensional Transition Metal Carbides and Nitrides. *Adv. Funct. Mater.* **2013**, *23*, 2185−2192.
(30) Kurtoglu, M.; Naguib, M.; Gogotsi, Y.; W.Barsoum, M. First Principles Study of Two-Dimensional Early Transition Metal Carbides. *MRS Commun.* **2012**, *2*, 133−137.
(31) Come, J.; Naguib, M.; Rozier, P.; Barsoum, M. W.; Gogotsi, Y.; Taberna, P. L.; Morcrette, M.; Simon, P. A Non-Aqueous Asymmetric Cell with a Ti_2C-Based Two-Dimensional Negative Electrode. *J. Electrochem. Soc.* **2012**, *159*, A1368−A1373.
(32) Kresse, G.; Furthmüller, J. Efficiency of ab-Initio Total Energy Calculations for Metals and Semiconductors Using a Plane-Wave Basis Set. *Comput. Mater. Sci.* **1996**, *6*, 15−50.
(33) Kresse, G.; Furthmüller, J. Efficient Iterative Schemes for ab-Initio Total-Energy Calculations Using a Plane-Wave Basis Set. *Phys. Rev. B* **1996**, *54*, 11169−11186.
(34) Kresse, G.; Joubert, J. From Ultrasoft Pseudopotentials to the Projector Augmented-Wave Method. *Phys. Rev. B* **1999**, *59*, 1758−1775.
(35) Wang, Y.; Perdew, J. P. Correlation Hole of the Spin-Polarized Electron Gas, with Exact Small-Wave-Vector and High-Density Scaling. *Phys. Rev. B* **1991**, *44*, 13298−13307.
(36) Grimme, S. Semiempirical GGA-type Density Functional Constructed with A Long-Range Dispersion Correction. *J. Comput. Chem.* **2006**, *30*, 1787−1799.
(37) Brandbyge, M.; Mozos, J. L.; Ordejon, P.; Taylor, J.; Stokbro, K. Density-Functional Method for Nonequilibrium Electron Transport. *Phys. Rev. B* **2002**, *65*, 165401.
(38) Cho, B.; Hahm, M. G.; Choi, M.; Yoon, J.; Kim, A. R.; Lee, Y. J.; Park, S. G.; Kwon, J. D.; Kim, C. S.; Song, M. K.; J, Y.; Nam, K. S.; Lee, S.; Yoo, T. J.; Kang, C. C.; Lee, B. H.; Ko, H. C.; Ajayan, P. M.; Kim, D. H. Charge-Transfer-Based Gas Sensing Using Atomic-Layer MoS_2. *Sci. Rep.* **2015**, *5*, 8052.
(39) Kou, L. Z.; Frauenheim, T.; Chen, C. F. Phosphorene as A Superior Gas Sensor: Selective Adsorption and Distince *I*−*V* Response. *J. Phys. Chem. Lett.* **2014**, *5*, 2675−2681.
(40) Cai, Y. Q.; Ke, Q. Q.; Zhang, G.; Zhang, Y. W. Energetics, Charge Transfer and Magnetism of Small Molecules Physisorbed on Phosphorene. *J. Phys. Chem. C* **2015**, *119*, 3102−3110.
(41) Guo, H. Y.; Zhang, W. H.; Lu, N.; Zhuo, Z. W.; Zeng, X. C.; Wu, X. J.; Yang, J. L. CO_2 Capture on h-BN Sheet with High Selectivity Controlled by External Electric Field. *J. Phys. Chem. C* **2015**, *119*, 6912−6917.
(42) Kou, L. Z.; Du, A. J.; Cheng, C. F.; Frauenheim, T. Strain Engineering of Selective Chemical Adsorption on Monolayer MoS_2. *Nanoscale* **2014**, *6*, 5156−5161.
(43) Tersoff, J.; Hamann, D. R. Theory and Application for the Scanning Tunneling Microscope. *Phys. Rev. Lett.* **1983**, *50*, 1998.

DOI: 10.1021/acsami.5b03737
ACS Appl. Mater. Interfaces 2015, 7, 13707−13713